Acoustic resonances in gas-filled spherical bulb with parabolic temperature profile

John P. Koulakis, Seth Pree and Seth Putterman

Citation: The Journal of the Acoustical Society of America **144**, 2847 (2018); doi: 10.1121/1.5078599
View online: https://doi.org/10.1121/1.5078599
View Table of Contents: https://asa.scitation.org/toc/jas/144/5
Published by the Acoustical Society of America

Acoustic resonances in gas-filled spherical bulb with parabolic temperature profile

John P. Koulakis,[a] Seth Pree, and Seth Putterman
Department of Physics and Astronomy, University of California Los Angeles, Los Angeles, California 90095, USA

(Received 10 August 2018; revised 19 October 2018; accepted 25 October 2018; published online 19 November 2018)

Acoustics is used to probe the temperature profile within a sulfur plasma lamp. A spherically symmetric temperature profile is assumed that drops with the square of the radius, consistent with a constant volumetric heating model. Acoustic resonance frequencies are calculated exactly in the case of an ideal gas. Experimental measurement of a few resonant frequencies allows determination of the temperature profile curvature. This technique can be viewed as an extension of ultrasonic resonant spectroscopy to systems that are highly non-uniform due to off-equilibrium energy flow.
 https://doi.org/10.1121/1.5078599

[VMK] Pages: 2847–2851

I. INTRODUCTION

The temperature of a gas-filled cavity of known geometry can be accurately measured by finding its acoustic resonance frequencies. Typically, such measurements are done under an assumed or approximate thermal equilibrium. When the gas is continuously heated, however, a steady-state, non-uniform temperature profile may form that changes the ratio of the resonant frequencies. Motivated by the conditions present in sulfur plasma lamps such as the one pictured in Fig. 1, we solve for the acoustic resonance spectrum of a sphere filled with an ideal gas whose temperature drops with the square of the radius. We have chosen a parabolic temperature variation because (1) it is the solution to Fourier's heating law for a sphere heated uniformly throughout its volume, (2) it is the first viable term of a perturbative expansion of a more general temperature profile, and (3) an analytic solution can be found for the acoustic eigenmodes.

Sulfur plasma lamps are well described in the literature.[1–5] The spherical bulbs are typically 3 cm in diameter and contain ∼30 mg sulfur. Microwaves heat the bulb until the sulfur vaporizes to a molecular density of about $10^{19}\,\mathrm{cm}^{-3}$ and an average temperature of about 2000 K. Rotation of the bulb at about 50 Hz suppresses convection and flickering, and homogenizes the fluid within.[5] While the low gas ionization fraction (about 10^{-5}) is critical for absorbing microwave energy, it does not affect sound propagation substantially. We therefore treat the bulb as being filled with neutral gas for acoustics purposes.

II. HEAT EQUATION WITH CONSTANT VOLUMETRIC HEATING

Sulfur plasma lamps are designed to efficiently convert microwave energy into visible light by thermally exciting radiative molecular transitions. The power not converted into visible light remains in the gas and causes further heating. This is the volumetric heat source, q (units of W cm^{-3}), in the following thermal analysis, which we take to be uniform throughout the bulb. Furthermore, as mentioned earlier, thermal convection due to gravity is suppressed by rotating the bulb,[5] so we only consider conductive heat transport in this analysis. Although gravity-driven convection is suppressed, a high-amplitude sound field can drive convection that dramatically impacts the temperature profile and resonances of the cavity.[6,7] Such high amplitudes only occur in the vicinity of a resonance. By searching for the resonances with a sweeping procedure outlined below, we are able to identify them in the quiescent bulb before the acoustically driven convection can appreciably affect it.

From the steady-state heat equation,

$$\nabla^2 T = -\frac{q}{\kappa}, \tag{1}$$

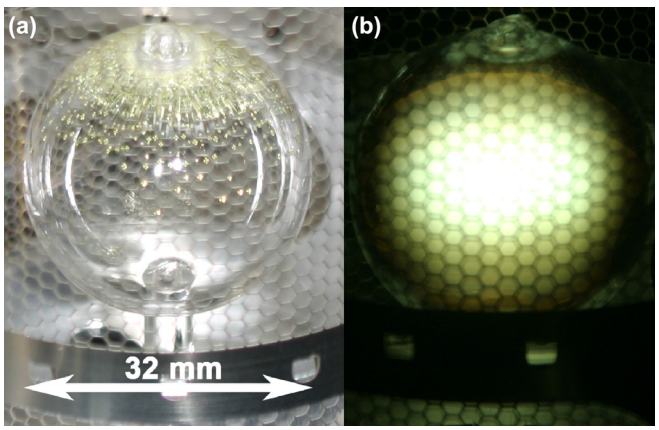

FIG. 1. (Color online) Sulfur plasma bulb shown while off (a) and on (b). The hexagonal metal mesh in the photographs is for containing the microwave field used to heat the bulb. Photograph (b) is taken through welding glass, resulting in the green tint. The ratios of the bulb's acoustic resonant frequencies shed light on the internal temperature profile.

[a]Electronic mail: koulakis@physics.ucla.edu

and boundary conditions $dT/dr|_{r=0} = 0$ and $T(r=0) = T_0$, we find that the temperature profile internal to the bulb is approximately parabolic.

$$T(r) = T_0\left(1 - \frac{q}{6\kappa T_0}r^2\right) = T_0\left(1 - \xi^2\frac{r^2}{R^2}\right), \tag{2}$$

where $\xi^2 = qR^2/(6\kappa T_0)$, R is the bulb radius, and we have taken the thermal conductivity κ to be constant with temperature. Our goal is to determine T_0 and ξ. Infrared thermometery can measure the temperature at the glass wall, $T_w = T_0(1-\xi^2)$, leaving one parameter to be determined by acoustics.

III. WAVE EQUATION IN AN INHOMOGENEOUS MEDIUM

The wave equation in an inhomogeneous medium is given by[8]

$$\nabla\cdot\left(\frac{\nabla p}{\rho}\right) - \frac{1}{\rho c^2}\frac{\partial^2 p}{\partial t^2} = 0, \quad \text{with} \quad \frac{\partial\vec{v}}{\partial t} = -\frac{1}{\rho}\nabla p, \tag{3}$$

where p and $\vec{v}$ are the acoustic pressure and velocity, and ρ and c are the spatially varying density and speed of sound, respectively. Approximating the hot sulfur gas as ideal, the speed of sound and density profiles are

$$c^2 = c_0^2\left(1 - \xi^2\frac{r^2}{R^2}\right), \quad \text{and} \quad \rho = \frac{\rho_0}{1-\xi^2\frac{r^2}{R^2}}, \tag{4}$$

where c_0 and ρ_0 are the speed of sound and density at the center of the bulb. Note that the quantity ρc^2 is independent of temperature for an ideal gas at constant pressure.

The solution is simplified by introducing the mass flux density potential[9] ψ,

$$\rho\vec{v} = \nabla\psi, \quad \text{with} \quad p = -\frac{\partial\psi}{\partial t}. \tag{5}$$

The wave equation for ψ becomes

$$\nabla^2\psi - \frac{1}{\rho}\nabla\rho\cdot\nabla\psi - \frac{1}{c^2}\frac{\partial^2\psi}{\partial t^2} = 0. \tag{6}$$

IV. EIGENMODES

Assuming harmonic time dependence at angular frequency ω and inserting the density and speed of sound profiles (4) into Eq. (6), the normal modes are given by the solutions of

$$\nabla^2\psi - \frac{2r\xi^2}{R^2\left(1-\xi^2\frac{r^2}{R^2}\right)}\nabla\psi + \frac{k_0^2}{1-\xi^2\frac{r^2}{R^2}}\psi = 0, \tag{7}$$

where $k_0 = \omega/c_0$. This equation can be solved analytically with separation of variables. The angular variation is given by the spherical harmonics, $\psi = f(r)Y_\ell^m(\theta,\phi)$. For the radial equation, we have

$$\frac{\partial^2 f}{\partial r^2} + \left[\frac{2}{r} - \frac{2r\xi^2}{R^2\left(1-\xi^2\frac{r^2}{R^2}\right)}\right]\frac{\partial f}{\partial r} + \left[\frac{k_0^2}{1-\xi^2\frac{r^2}{R^2}} - \frac{\ell(\ell+1)}{r^2}\right]f = 0. \tag{8}$$

Doing a change of variables to $z = \xi^2 r^2/R^2$,

$$z(1-z)\frac{\partial^2 f}{\partial z^2} + \left[\frac{3}{2} - \frac{5}{2}z\right]\frac{\partial f}{\partial z} + \left[\frac{k_0^2R^2}{4\xi^2} - \frac{\ell(\ell+1)}{4}\times\frac{(1-z)}{z}\right]f = 0. \tag{9}$$

Changing variables again to $F(z) = z^{-\ell/2}f(z)$ brings the equation to hypergeometric form,

$$z(1-z)\frac{\partial^2 F}{\partial z^2} + (c - (a+b+1)z)\frac{\partial F}{\partial z} - abF = 0, \tag{10}$$

with

$$a = \frac{3+2\ell}{4} + \left[\frac{1}{4}(\ell+3/2)^2 - \ell/2 + \frac{k_0^2R^2}{4\xi^2}\right]^{1/2}, \tag{11}$$

$$b = \frac{3+2\ell}{4} - \left[\frac{1}{4}(\ell+3/2)^2 - \ell/2 + \frac{k_0^2R^2}{4\xi^2}\right]^{1/2}, \tag{12}$$

and

$$c = 3/2 + \ell. \tag{13}$$

Since z varies between 0 and $\xi^2 < 1$, we pick solutions near the singular point $z = 0$. The independent solutions are the hypergeometric functions ${}_2F_1(a,\ b;\ c;\ z)$ and $z^{1-c}\,{}_2F_1(1+a-c, 1+b-c; 2-c; z)$, but to keep ψ (and the pressure) finite at $r = 0$, the second solution must be thrown out. The radial part of ψ is then

$$f(r) = A(\xi r/R)^\ell\,{}_2F_1\left(a,b,c,\frac{\xi^2r^2}{R^2}\right), \tag{14}$$

where A is a constant. Requiring zero radial velocity at the bulb radius, $r = R$, gives the eigenvalue equation,

$$2\ell\,{}_2\tilde{F}_1(a,b;c;\xi^2) + (2\ell\xi^2 - k_0^2R^2)\,{}_2\tilde{F}_1 \times (a+1, b+1; c+1; \xi^2) = 0, \tag{15}$$

where ${}_2\tilde{F}_1(a,b;c;z) = {}_2F_1(a,b;c;z)/\Gamma(c)$ are the regularized hypergeometric functions. The solutions to the eigenvalue equation are the dimensionless resonant frequencies $k_{\ell,n}R = \omega_{\ell,n}R/c_0$ and are plotted as a function of ξ in Fig. 2(a). In the limit of thermal equilibrium, $\xi \to 0$, the standard acoustic resonances of homogeneous gas in a spherical cavity[10,11] are obtained. As ξ increases, the resonant frequencies drop and, crucially for our purposes, their ratios change. To

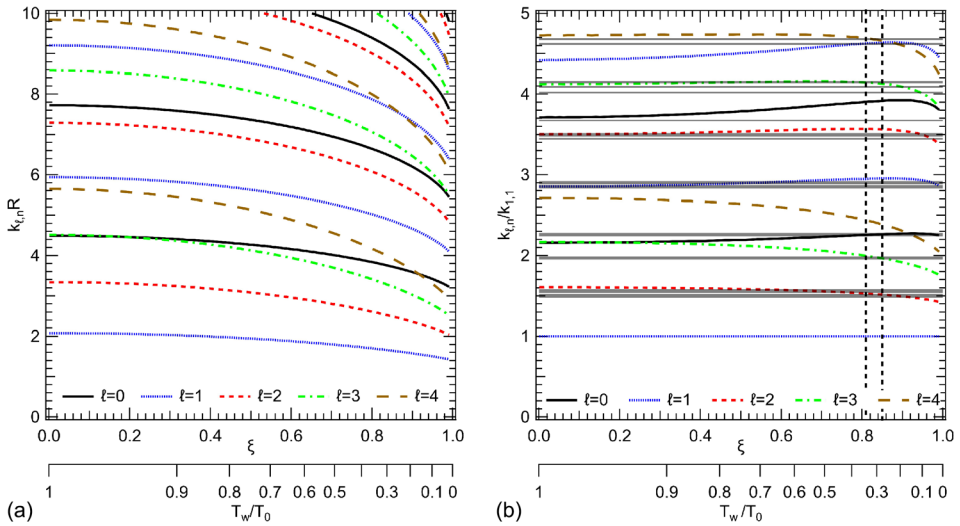

FIG. 2. (Color online) Dimensionless resonant frequencies as a function of the strength of the parabolic radial variation of the temperature, ξ (a). The vertical axis is $k_{\ell,n}R = \omega_{\ell,n}R/c_0$. Normalizing by the lowest frequency mode (b) allows using the resonant spectrum to determine ξ. Gray bands in (b) are the 95% confidence interval of the experimentally measured normalized resonant frequencies listed in Table I, which determine ξ in our system to be between the two vertical dashed lines.

demonstrate how the varying temperature affects the modes, we plot the $\ell = 0$ modes for various ξ in Fig. 3. The main effect is to shift the position of the nodes towards the outer boundary, as might be expected from the higher speed of sound near the center, and to increase the amplitude in the outer regions compared to the inner ones. Some readers might be surprised that the $\ell = 0$ mode does not have the lowest resonant frequency. This is crudely understood by considering that fluid traveling in an angular direction ($\ell \neq 0$) has the opportunity to go further than fluid traveling purely radially ($\ell = 0$), and so the wavelength of angular modes can be larger.[12]

V. EXPERIMENTAL DETERMINATION OF THE TEMPERATURE VARIATION IN A PLASMA BULB

We have modified an off-the-shelf plasma lamp to allow pulsing of the microwave power supply[13,14] at frequencies between 5 and 75 kHz. The periodic heating excites sound waves inside the bulb[15,16] that modulate the light emission. As

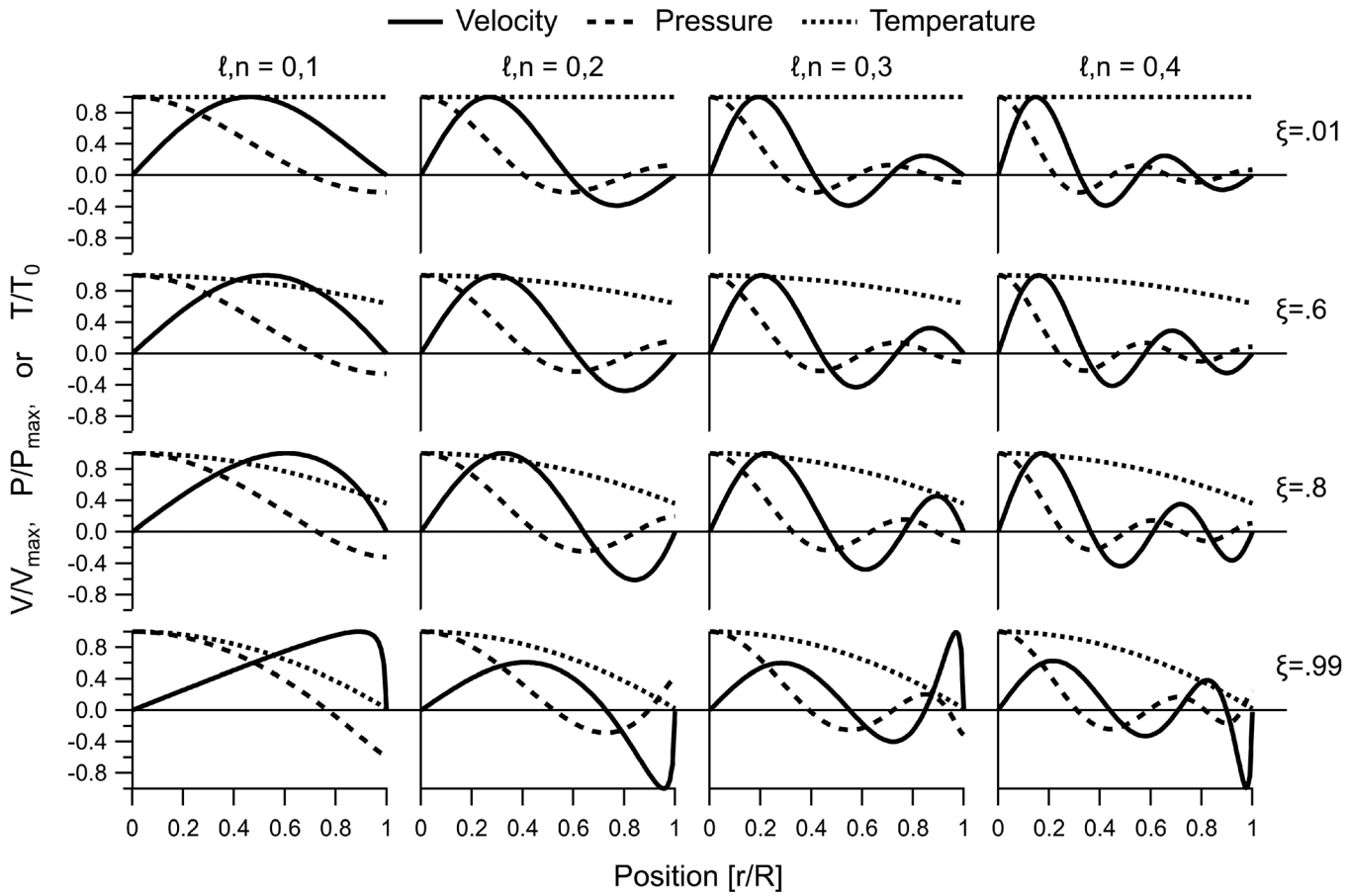

FIG. 3. $\ell = 0$ modes for various ξ. The main effect of the parabolic temperature profile is to shift the nodes towards the glass and to increase the acoustic amplitude in the outer regions relative to the inner ones.

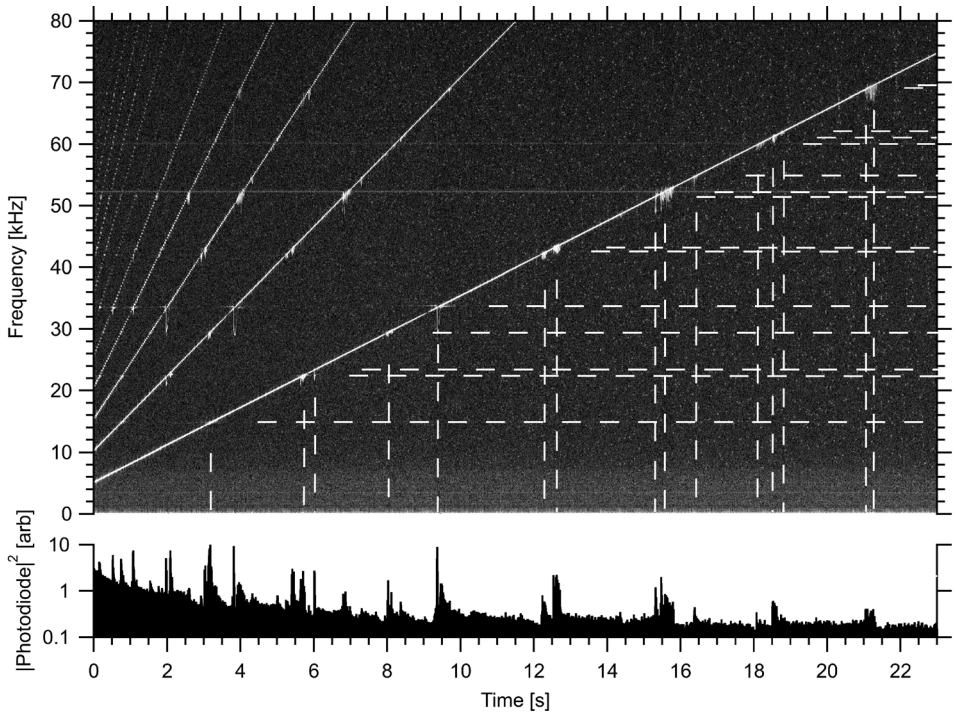

FIG. 4. The high-pass-filtered photodiode signal during a sweep of the pulse frequency between 5 and 75 kHz allows identification of the lowest acoustic resonant frequencies listed in Table I. Its squared magnitude is plotted on a logarithmic scale to easily identify times of large AC response. The spectrogram allows distinguishing a response at the drive frequency itself from a response at harmonics of the drive frequency. The lowest oblique line is at the fundamental drive frequency and resonant responses falling on this line are indicated by the vertical and horizontal dashed white lines. The higher, steeper lines are the drive harmonics and demonstrate that integer multiples of the drive can also excite the resonances. For example, the peaks in the photodiode signal at times less than 3 s were at harmonics of the drive. The stalactite-like chirps that can be seen dropping from the drive frequency at the onset of most resonances are indicative of the acoustically driven convection referenced in the text.

the pulse frequency is swept, acoustic resonances are easily identified on a photodiode trace. Figure 4 displays the high-pass-filtered photodiode signal and its spectrogram during a frequency sweep from 5 to 75 kHz over 23 s. Away from a resonance, the photodiode has a low-amplitude, sawtooth-shaped AC component[6,17] in phase with the pulse frequency. Near resonance the AC amplitude increases dramatically, becomes sinusoidal, and has two frequency components—one at the drive frequency and one that varies but remains within 1 kHz of the drive frequency as described and explained elsewhere.[6,7,17] Resonant frequencies are indicated by the dashed lines on the spectrogram and are listed in Table I. Evidently, non-sphericity in the bulb splits the degeneracy of the different m modes at a given ℓ, some of which can be resolved. Normalizing the resonant frequencies by the lowest one and comparing to Fig. 2(b) determines $\xi = 0.835 \pm 0.025$ and the temperature profile in the bulb. Using a FLIR-T400/HT ThermaCAM infrared camera we have measured the quartz temperature to be $T_w = 1250 \pm 100$ K, which when combined with knowledge of ξ gives the core temperature $T_0 = T_w/(1-\xi^2) = 4200 \pm 600$ K. The heat conducted out of the bulb is $4\pi R^2 \kappa (\partial T/\partial r)_R = 8\pi R \kappa T_w \xi^2/(1-\xi^2) = 470 \pm 260$ W. In arriving at these results, we have taken the emissivity of quartz[18,19] to be 0.65 ± 0.1 at 1250 K, and the thermal conductivity of the hot sulfur gas[20] to be 0.4 ± 0.2 W m^{-1} K^{-1}.

VI. DISCUSSION AND CONCLUSION

While the methods outlined above describe an approach to measuring the temperature profile within a spherical plasma bulb, they rely on simplifying assumptions which may not be justified. Specifically, the thermal conductivity does vary with the square root of temperature for an ideal gas, and in a more complicated way in a molecular plasma.[20] The volumetric heating rate, q, in the actual bulb is the difference between microwave absorption and visible light emission, which is spatially varying and a strong function of temperature. More

TABLE I. Acoustic resonant frequencies observed in a 32 mm diameter spherical plasma bulb. The normalized values are plotted as bands in Fig. 2(b) to allow determination of ξ. Splitting of some $\ell \neq 0$ modes is caused by the deviation from spherical symmetry in the actual bulb.

Mode (l, n)	Experimental res. freq. [kHz]	Normalized res. freq.
1, 1	14.9 ± 0.2	1
2, 1	22.4 ± 0.2	1.50 ± 0.012
2, 1	23.3 ± 0.2	1.56 ± 0.012
3, 1	29.5 ± 0.2	1.97 ± 0.01
0, 1	33.7 ± 0.2	2.26 ± 0.01
1, 2	42.5 ± 0.4	2.85 ± 0.01
1, 2	43.3 ± 0.4	2.90 ± 0.01
2, 2	51.5 ± 0.2	3.445 ± 0.005
2, 2	52.2 ± 0.4	3.495 ± 0.01
2, 2	54.9 ± 0.2	3.675 ± 0.005
3, 2	60.1 ± 0.3	4.020 ± 0.006
3, 2	61.2 ± 0.2	4.090 ± 0.005
3, 2	62.1 ± 0.4	4.150 ± 0.007
1, 3	69.0 ± 0.4	4.620 ± 0.006
1, 3	69.9 ± 0.4	4.680 ± 0.006

accurate solutions to the heat equation may be used as the starting point for the eigenvalue calculations, but an analytical form of the eigenvalue equation may not be possible. In that case the prescribed procedure can be executed using numerical eigenvalue calculations as needed. Resolving more detail in the temperature profile will require extending the resonant frequency measurement to higher modes. Due to buoyancy of the warm gas and rotation of the bulb,[5] the temperature variation is not spherically symmetric, resulting in the splitting of the degeneracy for different m modes of the same ℓ, an effect that is not addressed by the current theoretical treatment. Nonetheless, these acoustic methods have allowed us to measure parameters for an approximate thermal model and estimate the core temperature and heat conducted to the boundary.

Laboratory plasmas are intrinsically off equilibrium systems. In addition to temperature, key parameters include the degree of ionization. We hope that this method can be extended to the regions of parameter space where signatures of ion acoustic modes will appear.

ACKNOWLEDGMENTS

This material is based upon work supported by the Air Force Office of Scientific Research under award number FA9550-16-1-0271.

[1]J. T. Dolan, M. G. Ury, and C. H. Wood, "A novel high efficacy microwave powered light source," in *The Sixth International Symposium on the Science and Technology of Light Sources (Lighting Sciences* 6), edited by L. Bartha and F. J. Kedves (Technical University of Budapest, Hungary, 1992), pp. 301–302.
[2]J. T. Dolan, M. G. Ury, and C. H. Wood, "Lamp including sulfur," U.S. patent 5404076 A (April 4, 1995).
[3]C. W. Johnston, H. W. P. van der Heijden, G. M. Janssen, J. van Dijk, and J. J. A. M. van der Mullen, "A self-consistent LTE model of a microwave-driven, high pressure sulfur lamp," J. Phys. D: Appl. Phys **35**(4), 342–351 (2002).
[4]C. W. Johnston, H. W. P. van der Heijden, A. Hartgers, K. Garloff, J. van Dijk, and J. J. A. M. van der Mullen, "An improved LTE model of a high pressure sulfur lamp," J. Phys. D: Appl. Phys **37**(2), 211–220 (2004).
[5]B. P. Turner, M. G. Ury, Y. Leng, and W. G. Love, "Sulfur lamps—Progress in their development," J. Illum. Eng. Soc. **26**(1), 10–16 (1997).
[6]J. P. Koulakis, S. Pree, A. L. F. Thornton, and S. Putterman, "Trapping of plasma enabled by pycnoclinic acoustic force," Phys. Rev. E **98**(4), 043103 (2018).
[7]S. Pree, J. Koulakis, A. Thornton, and S. Putterman, "Acousto-convective relaxation oscillation in plasma lamp," Proc. Mtgs. Acoust. **34**, 045015 (2018).
[8]L. D. Landau and E. M. Lifshitz, *Course of Theoretical Physics: Fluid Mechanics*, 2nd ed. (Elsevier, Oxford, UK), Vol. 6, Chap. 76, p. 292.
[9]P. Collas and M. Barmatz, "Acoustic radiation force on a particle in a temperature gradient," J. Acoust. Soc. Am. **81**(5), 1327–1330 (1987).
[10]D. A. Russell, "Basketballs as spherical acoustic cavities," Am. J. Phys. **78**(6), 549–554 (2010).
[11]M. R. Moldover, J. B. Mehl, and M. Greenspan, "Gas-filled spherical resonators: Theory and experiment," J. Acoust. Soc. Am. **79**(2), 253–272 (1986).
[12]L. Kinsler, A. R. Frey, A. B. Coppens, and J. V. Sanders, *Fundamentals of Acoustics*, 4th ed. (Wiley, New York, 2000), pp. 250–252.
[13]S. Gavin, M. Carpita, and G. Courret, "Power electronics for a sulfur plasma lamp working by acoustic resonance: Full scale prototype experimental results," in *16th European Conference on Power Electronics and Applications* (IEEE, New York, 2014).
[14]J. P. Koulakis, A. L. F. Thornton, and S. Putterman, "Magnetron coupling to sulfur plasma bulb," IEEE Trans. Plasma Sci. **45**(11), 2940–2944 (2017).
[15]U. Ingard, "Acoustic wave generation and amplification in a plasma," Phys. Rev. **145**(1), 41–45 (1966).
[16]A. K. Mohanty and C. C. Oliver, "Acoustic waves in pulsed microwave discharges," J. Phys. D: Appl. Phys. **8**(10), 1202–1205 (1975).
[17]G. Courret, P. Nikkola, S. Wasterlain, O. Gudozhnik, M. Girardin, J. Braun, S. Gavin, M. Croci, and P. W. Egolf, "On the plasma confinement by acoustic resonance—An innovation for electrodeless high-pressure discharge lamps," Eur. Phys. J. D **71**(8), 214 (2017).
[18]R. M. Sova, M. J. Linevsky, M. E. Thomas, and F. F. Mark, "High-temperature infrared properties of sapphire, AlON, fused silica, yttria, and spinel," Infrared Phys. Technol. **39**(4), 251–261 (1998).
[19]J. R. Markham, P. R. Solomon, and P. E. Best, "An FT-IR based instrument for measuring spectral emittance of material at high temperature," Rev. Sci. Instrum. **61**(12), 3700–3708 (1990).
[20]C. Johnston, "Transport and equilibrium in molecular plasmas: The sulfur lamp," Ph.D. thesis, Technische Universiteit Eindhoven, Eindhoven, 2003.